nature neuroscience

OSVZ progenitors of human and ferret neocortex are epithelial-like and expand by integrin signaling

Simone A Fietz[1], Iva Kelava[1], Johannes Vogt[2], Michaela Wilsch-Bräuninger[1], Denise Stenzel[1], Jennifer L Fish[1], Denis Corbeil[3], Axel Riehn[4], Wolfgang Distler[4], Robert Nitsch[2] & Wieland B Huttner[1]

A major cause of the cerebral cortex expansion that occurred during evolution is the increase in subventricular zone (SVZ) progenitors. We found that progenitors in the outer SVZ (OSVZ) of developing human neocortex retain features of radial glia, in contrast to rodent SVZ progenitors, which have limited proliferation potential. Although delaminating from apical adherens junctions, OSVZ progenitors maintained a basal process contacting the basal lamina, a canonical epithelial property. OSVZ progenitor divisions resulted in asymmetric inheritance of their basal process. Notably, OSVZ progenitors are also found in the ferret, a gyrencephalic nonprimate. Functional disruption of integrins, expressed on the basal process of ferret OSVZ progenitors, markedly decreased the OSVZ progenitor population size, but not that of other, process-lacking SVZ progenitors, in slice cultures of ferret neocortex. Our findings suggest that maintenance of this epithelial property allows integrin-mediated, repeated asymmetric divisions of OSVZ progenitors, providing a basis for neocortical expansion.

Cortical expansion is a hallmark of mammalian brain evolution. A major underlying cause of this expansion is the increase in the population size of neural progenitors and in the number of neurogenic divisions that they undergo during cortical development[1–5]. Two principal classes of neural progenitors exist in the developing cortex[6,7]. The first comprises neuroepithelial cells and the radial glial cells (RGCs) that they transform into with the onset of neurogenesis. These progenitors, which exhibit characteristics of neural stem cells, show apical-basal cell polarity and span the cortical wall from the basal lamina (pia) to the ventricular (apical) surface, with their cell bodies occupying the apical-most layer of the cortical wall, the ventricular zone. These ventricular zone progenitors are connected by adherens junctions at the apical-most end of their lateral plasma membrane, and their primary cilium protrudes from the apical plasma membrane into the ventricular lumen. The resulting apical localization of their centrosomes leads to their mitosis occurring at the ventricular surface, which is why these progenitors have also been collectively referred to as apical progenitors. Their mitosis is followed by interkinetic nuclear migration, that is, the apical-to-basal movement of their nuclei in G1 for S phase at an abventricular location and the basal-to-apical movement of their nuclei in G2 for the next mitosis. Interkinetic nuclear migration underlies the pseudostratified appearance of the ventricular zone[4,7].

The second class of neural progenitors in the developing cortex, which have mostly been studied in rodents, are cells that are born from apical progenitors in the ventricular zone, but that delaminate from the apical belt of adherens junctions and migrate in the basal direction to form, and to typically divide in, a second, more basal progenitor layer, the SVZ[1,6]. In rodents, these progenitors retract their apical and basal processes during their cell cycle, lose their apical-basal polarity by M phase, and, in most instances, divide only once to generate two neurons[1,6,8]. Given their basal location and intermediate nature in the lineage from apical progenitors to neurons, these progenitors have been referred to as basal[6] or intermediate[1] progenitors.

Apical progenitors expand by symmetric proliferative divisions. This determines the size of the primary progenitor population and the number of radial units[5]. Spatial accommodation of the increasing number of apical progenitors is achieved by them becoming very elongated, which in turn increases the degree of pseudostratification of the ventricular zone[4]. In addition, this proliferation results in the lateral expansion of the ventricular zone[5].

It is, however, the expansion of the SVZ that constitutes the most notable difference between mammals that show various degrees of cortical expansion[1,3,4]. As the proliferative potential of rodent basal progenitors is very limited[1,6], in contrast to that of apical progenitors, the question arises whether this could be a result of differences in the cell biology of these progenitors. A corollary of this consideration is whether SVZ progenitors in species developing a gyrencephalic cortex, a cortex with a laterally expanded, folded pial surface, have cell biological features that are distinct from their counterparts in species with a lissencephalic, smooth cortical surface, such as rodents.

A crucial observation in this regard has been the description of a unique germinal layer in the monkey, referred to as OSVZ[9]. A characteristic morphological feature of the monkey OSVZ, in comparison with the rodent SVZ, is its radial appearance, which has led to the suggestion that the OSVZ may harbor RGC cell bodies[9]. Extending this to the cell

[1]Max Planck Institute of Molecular Cell Biology and Genetics, Dresden, Germany. [2]Institute of Cell Biology and Neurobiology, Center for Anatomy, Charité, Berlin, Germany. [3]BIOTEC, Technische Universität Dresden, Dresden, Germany. [4]Klinik und Poliklinik für Frauenheilkunde und Geburtshilfe, Universitätsklinikum Carl Gustav Carus, Technische Universität Dresden, Dresden, Germany. Correspondence should be addressed to W.B.H. (huttner@mpi-cbg.de).

Received 9 February; accepted 19 April; published online 2 May 2010; doi:10.1038/nn.2553

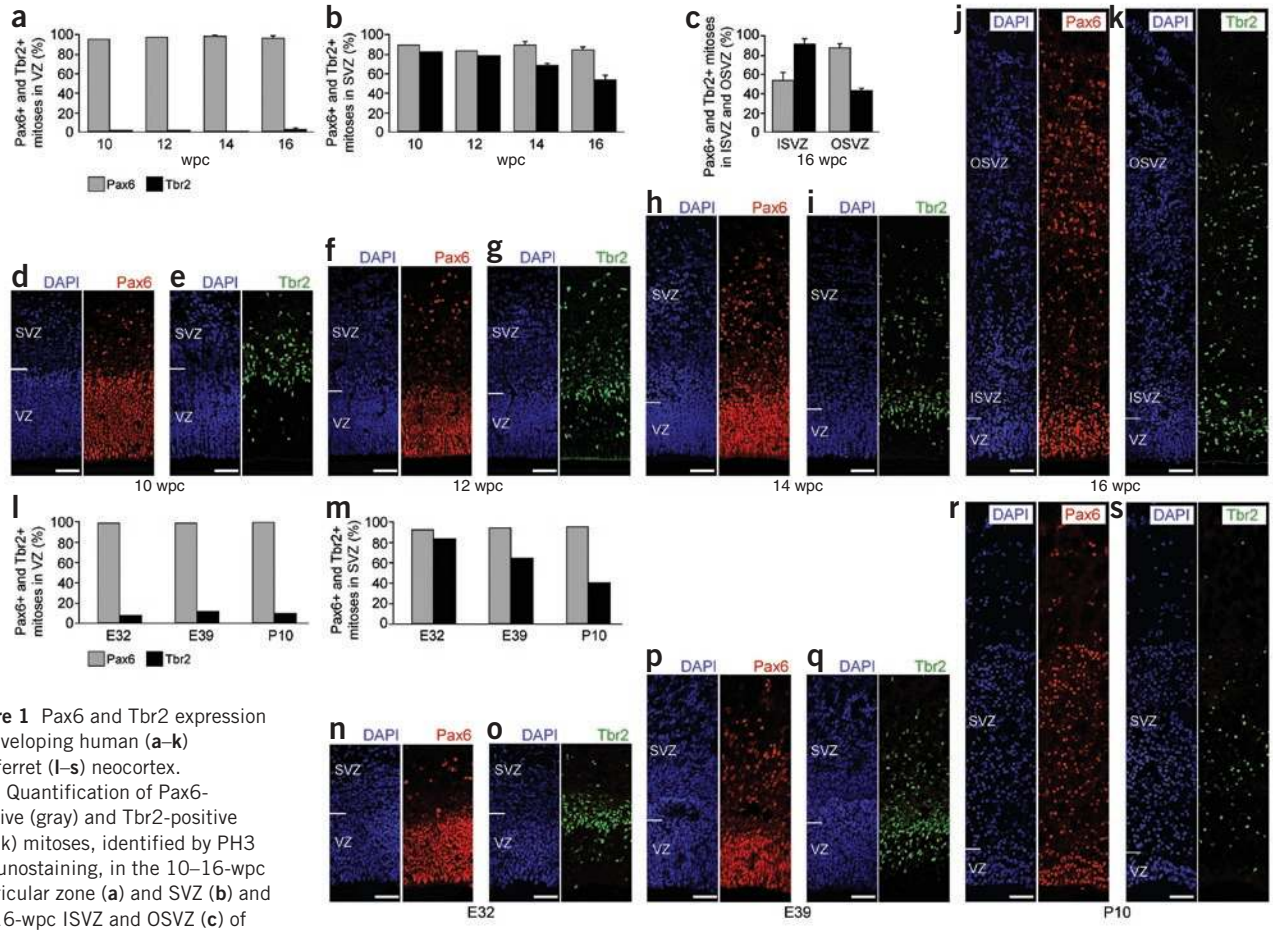

Figure 1 Pax6 and Tbr2 expression in developing human (**a**–**k**) and ferret (**l**–**s**) neocortex. (**a**–**c**) Quantification of Pax6-positive (gray) and Tbr2-positive (black) mitoses, identified by PH3 immunostaining, in the 10–16-wpc ventricular zone (**a**) and SVZ (**b**) and the 16-wpc ISVZ and OSVZ (**c**) of human fetal neocortex, expressed as the percentage of total PH3-positive cells in the respective layer (**Supplementary Text**). Data for 10- and 12-wpc are from one fetus and data for 14- and 16-wpc are from two fetuses; bars indicate variation of individual values from the mean. VZ, ventricular zone. (**d**–**k**) Pax6 (red), Tbr2 (green) and DAPI (blue) staining on cryosections (**d**,**e**; paraformaldehyde, PFA) and paraffin sections (**f**–**k**; formalin) of 10–16-wpc human fetal neocortex. The basal boundary of the SVZ and OSVZ corresponds to the top margin of the images. Scale bars represent 50 μm. (**l**,**m**) Quantification of Pax6-positive (gray) and Tbr2-positive (black) mitoses, identified by PH3 immunostaining, in the ventricular zone (**l**) and SVZ (**m**) of E32–P10 ferret neocortex, expressed as the percentage of total PH3-positive cells in the respective layer (**Supplementary Text**). Data are from one developing ferret brain each. (**n**–**s**) Pax6 (red), Tbr2 (green) and DAPI (blue) staining on cryosections of PFA-fixed E32–P10 ferret neocortex. Data are presented as in **d**–**k**.

biological level, we previously hypothesized that OSVZ progenitors maintain certain epithelial features and that it is this maintenance that endows them with the capacity for self-renewal and that is required for OSVZ expansion (epithelial progenitor hypothesis)[4]. We investigated this hypothesis and found that OSVZ progenitors exist not only in primates, notably human, but also in a nonprimate species that develops a gyrencephalic cortex, the ferret, with the branch point in the phylogenetic tree for these two species dating back 97 million years[10]. OSVZ progenitors maintained contact with the basal lamina throughout their cell cycle via retention of a basal process, a canonical epithelial feature. Moreover, we found that integrin function was required to ensure the full population size of these basal process–bearing OSVZ progenitors.

RESULTS

Human OSVZ progenitors exhibit characteristics of RGCs

To define the molecular nature of human OSVZ progenitors, we first considered the abventricular location of their nuclei and determined whether they expressed Tbr2, a transcription factor that is expressed in SVZ progenitors in rodents[11,12] (**Fig. 1**). Consistent with previous findings[13], Tbr2 immunoreactivity was much more pronounced in the SVZ than in the ventricular zone of 10-week-old human neocortex (**Fig. 1e**). As the human SVZ developed and the distinct ISVZ and OSVZ emerged at 12–16 weeks post-conception (wpc), Tbr2 was more prominently expressed in the human ISVZ than in the OSVZ (**Fig. 1g**,**i**,**k**). This suggests that human ISVZ progenitors are more related to rodent SVZ progenitors than is the case for human OSVZ progenitors and raises the possibility that OSVZ progenitors might have features that are not typically observed for rodent SVZ progenitors.

We then examined the expression of Pax6, a transcription factor that is expressed in rodent ventricular zone progenitors, but downregulated in rodent SVZ progenitors[4,11,12,14]. At 10 wpc, as in rodents, Pax6 was abundantly expressed in the human ventricular zone, but sparsely expressed in the SVZ (**Fig. 1d**), a marked difference from the expression of Tbr2 in these two germinal layers (**Fig. 1e**). Concomitant with the emergence of the human OSVZ during 12–16 wpc, Pax6-positive nuclei progressively appeared in the OSVZ, seemingly at the expense of the ventricular zone, which became thinner (**Fig. 1f**,**h**,**j**). These data confirm and extend previous reports on the expression of Pax6 in primate OSVZ[4,13,15] and suggest a close relationship between OSVZ and ventricular zone progenitors.

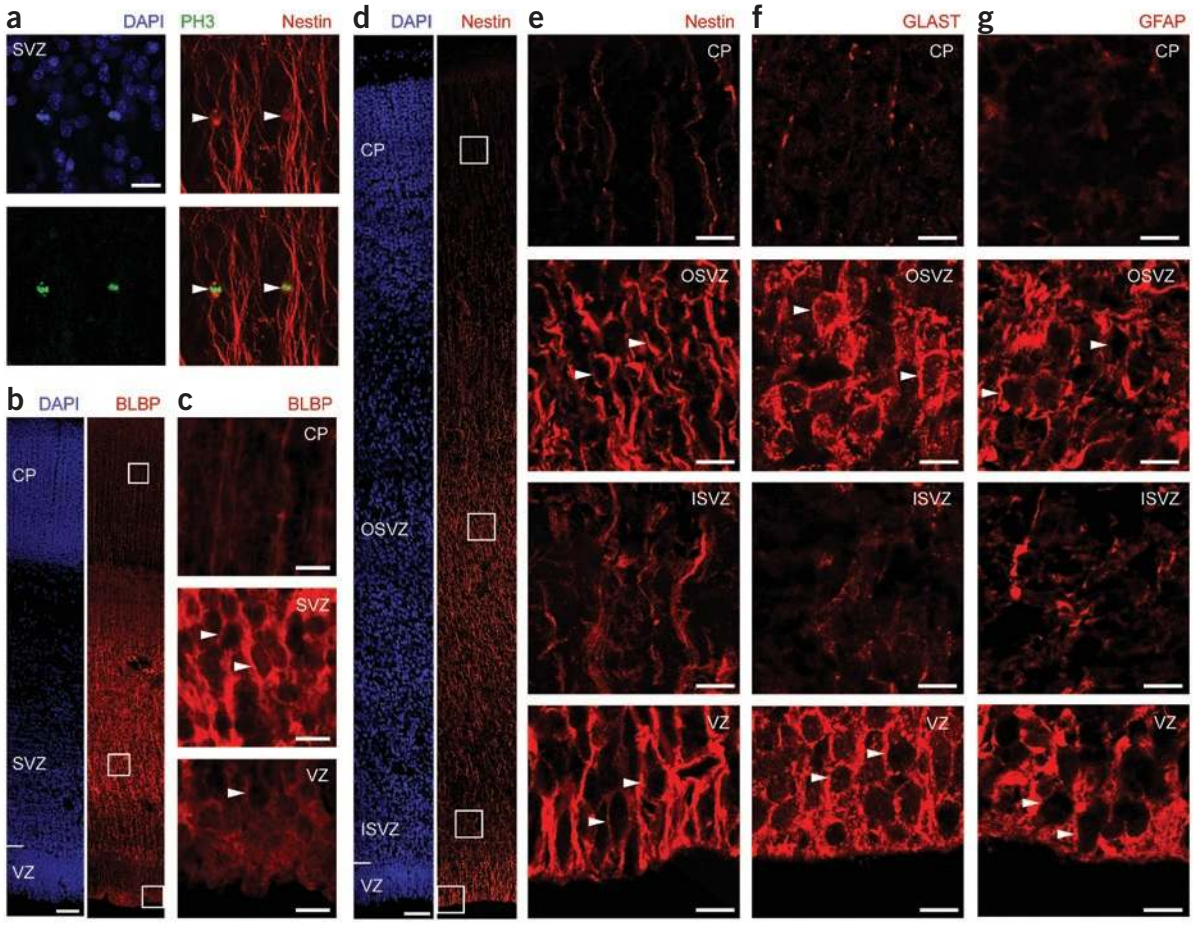

Figure 2 Human OSVZ progenitors express markers of radial glia. (**a**) Double immunofluorescence for nestin (red) and PH3 (green) on a vibratome section of 11-wpc human fetal neocortex (PFA). DAPI staining is shown in blue. A portion of the SVZ is shown (stack of eight optical sections). Arrowheads indicate mitotic SVZ progenitor cell bodies showing nestin immunoreactivity. Scale bar represents 10 μm. (**b**,**c**) Immunofluorescence for BLBP (red) on a vibratome section of 13-wpc human fetal neocortex (PFA). DAPI staining is shown in blue. Boxed areas in **b** are shown at higher magnification in **c**. Arrowheads indicate cell body–associated BLBP immunoreactivity in the SVZ and ventricular zone. Scale bars represent 50 μm (**b**) and 10 μm (**c**). (**d**–**g**) Immunofluorescence (red) for nestin (**d**,**e**), GLAST (**f**) and GFAP (**g**) on paraffin sections of 16-wpc human fetal neocortex (formalin). DAPI staining is shown in blue. Boxed areas in **d** are shown at higher magnification in **e** and are representative of the areas shown in **f** and **g**. Arrowheads indicate cell body–associated immunoreactivity in the OSVZ and ventricular zone. Scale bars represent 50 μm (**d**) and 10 μm (**e**–**g**). CP, cortical plate.

To corroborate the progenitor nature of the Pax6- and Tbr2-positive cells in the human ventricular zone, SVZ and, when discernible, ISVZ and OSVZ, and to obtain quantitative data, we confined our analysis to mitotic cells, as determined by phosphohistone H3 (PH3) immunostaining. At 10 wpc, consistent with previous observations[16], the location of mitotic figures was similar to that seen in rodents at early stages of neurogenesis, with the vast majority being found at the ventricular surface, whereas the relative increase in mitotic figures in the human SVZ, in comparison with the mouse SVZ, became evident at later stages (data not shown). At any of the developmental stages examined, >95% of progenitors in the ventricular zone expressed Pax6 (**Fig. 1a**), whereas <5% of them expressed Tbr2 (**Fig. 1a**). Pax6 was expressed in the majority (>80%) of progenitors in the human SVZ (**Fig. 1b**). Separate analysis of the ISVZ and OSVZ at 16 wpc revealed that only about half of the progenitors in the ISVZ expressed Pax6, whereas ≈90% of progenitors in the OSVZ expressed Pax6 (**Fig. 1c**). The proportion of progenitors expressing Tbr2 in the human SVZ decreased from >80% at 10 wpc to <60% at 16 wpc (**Fig. 1b**). Separate analysis of the ISVZ and OSVZ at 16 wpc revealed that, conversely to Pax6, almost all progenitors in the ISVZ, but less than half of the progenitors in the OSVZ, expressed Tbr2 (**Fig. 1c**). Together, these data suggest the existence of at least two progenitor subpopulations in the human SVZ, ISVZ progenitors that express Tbr2, but downregulate Pax6 expression, and resemble rodent basal progenitors, and OSVZ progenitors that do not generally sustain Tbr2 expression, but, similarly to ventricular zone progenitors, maintain Pax6 expression and have no counterpart in the rodent SVZ.

These observations prompted us to ask whether other, cytoplasmic markers expressed in ventricular zone progenitors are expressed in human OZVZ progenitors. Specifically, we looked for nestin, which is expressed in neuroepithelial cells and RGCs[17], brain lipid–binding protein (BLBP) and GLAST, two proteins that are expressed in ventricular zone progenitors after their transformation into RGCs[17], and GFAP, which is expressed in primate[18], but not in early rodent[19], RGCs. We detected all four proteins not only in the human ventricular zone, but also OSVZ at 11–16 wpc (**Fig. 2**). In either germinal layer, all four proteins, notably nestin (**Fig. 2a**), were expressed not only in traversing radial fibers, as was the case for the ISVZ, but also in the cell body cytoplasm (**Fig. 2a**,**c**,**e**–**g**), indicating that they were expressed in ventricular zone and OSVZ progenitors. This was corroborated for SVZ progenitors by staining for both nestin and PH3 (**Fig. 2a**). These data indicate that human OSVZ progenitors, in

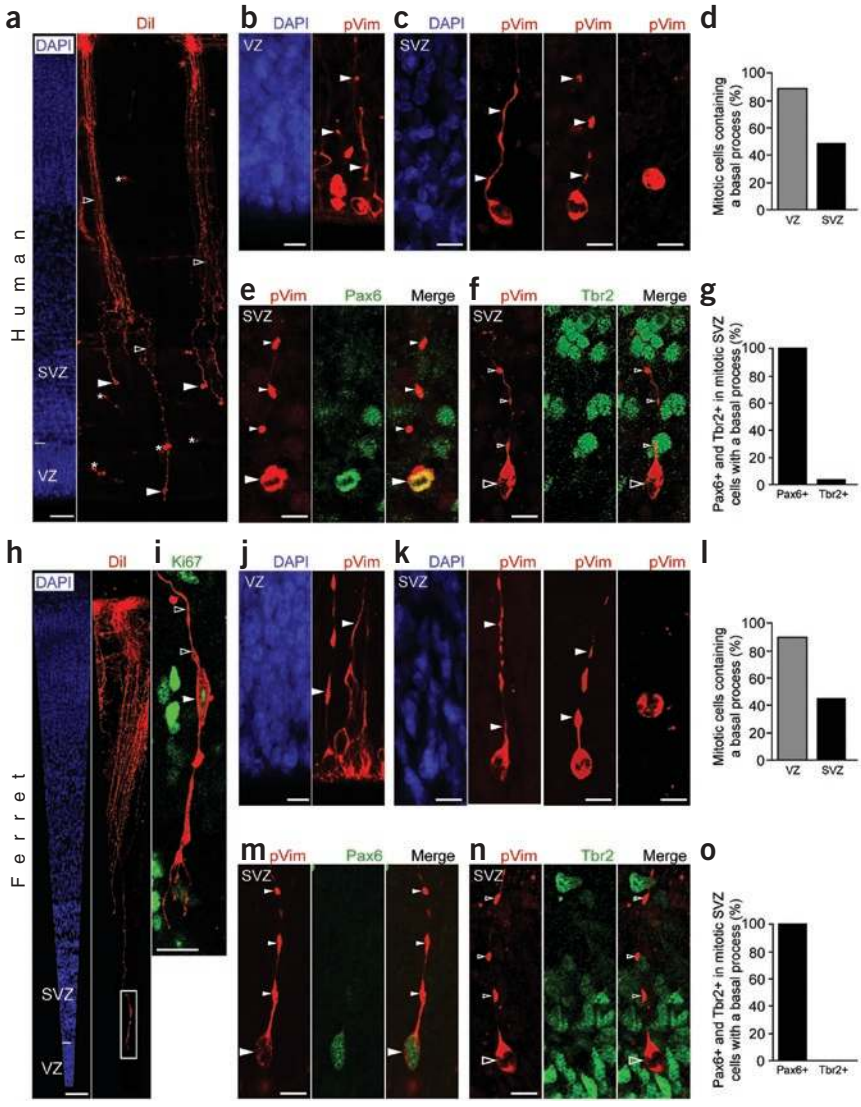

Figure 3 Human and ferret OSVZ progenitors retain basal processes through M phase. (**a**–**g**) 13-wpc human fetal neocortex (PFA): vibratome sections (**a**–**d**) and cryosections (**e**–**g**). (**a**) DiI labeling (red) from the pial surface of the cortical wall (stack of 28 optical sections). DAPI staining is shown in blue. Solid arrowheads indicate DiI-labeled cell bodies, open arrowheads indicate DiI-labeled cellular processes and asterisks indicate autofluorescent blood vessels. The DAPI image corresponds to a segment of the DiI image. Scale bar represents 50 μm. (**b**,**c**) Immunofluorescence for phosphovimentin (pVim, red) in the human ventricular zone (**b**) and SVZ (**c**) (stacks of 6–12 optical sections). DAPI staining is shown in blue. Arrowheads indicate phosphovimentin-positive basal processes. Scale bars represent 5 μm. (**d**) Quantification of the percentage of mitotic progenitors by phosphovimentin immunostaining in the human ventricular zone (gray columns) and SVZ (black columns) that had phosphovimentin-positive basal processes (**Supplementary Text**). Data are from one human fetus. (**e**,**f**) Double immunofluorescence for phosphovimentin (pVim, red) and either Pax6 (**e**, green) or Tbr2 (**f**, green) in human SVZ progenitors (stacks of 5–8 optical sections). Solid arrowheads indicate Pax6-positive mitotic SVZ progenitors extending a basal process. Open arrowheads indicate Tbr2-negative mitotic human SVZ progenitors extending a basal process. Scale bars represent 5 μm. (**g**) Quantification of the percentage of mitotic, basal process–bearing human SVZ progenitors, identified by phosphovimentin immunostaining, that expressed either Pax6 or Tbr2 (**Supplementary Text**). Data are from one human fetus. (**h**–**o**) E39 ferret neocortex (PFA, vibratome sections). (**h**,**i**) DiI labeling (red) from the pial surface of the cortical wall, combined with Ki67 immunofluorescence (**i**, green) and DAPI staining (**h**, blue); stack of 20 optical sections. The boxed area in **h** is shown at higher magnification in **i**. Solid arrowheads indicate a DiI-labeled Ki67-positive cell body. Open arrowheads indicate a DiI-labeled basal process. Scale bar represents 50 μm (**h**) and 20 μm (**i**). (**j**,**k**) Data are presented as in **b** and **c** for ferret ventricular zone (**j**) and SVZ (**k**) (stacks of 7–12 optical sections). Scale bars represent 5 μm. (**l**) Data are presented as in **d** for ferret ventricular zone and SVZ. Data are from one ferret embryo. (**m**,**n**) Data are presented as in **e** and **f** for ferret SVZ progenitors. Scale bars represent 5 μm. (**o**) Data are presented as in **g** for ferret SVZ progenitors. Data are from one ferret embryo.

contrast to rodent basal progenitors, maintain expression of cytoplasmic markers of ventricular zone progenitors and are more closely related to these progenitors than rodent basal progenitors.

Human OSVZ progenitors retain a basal process in M phase

Rodent apical progenitors retain their basal processes through M phase[20–22], whereas rodent basal progenitors in M phase lack processes of any substantial length[8]. Given the close relationship between human OSVZ and ventricular zone progenitors with regard to molecular marker expression and the presence of a basal process in monkey OSVZ progenitors during interphase[23], we investigated whether human OSVZ progenitors retained basal processes through M phase (**Fig. 3**). DiI (1,1′-dioctadecyl-3,3,3′,3′-tetramethylindocarbocyanine perchlorate) labeling from the pial side of 13-wpc human cortical sections revealed the presence of processes that extended from the pial surface to cell bodies residing in the OSVZ and ventricular zone (**Fig. 3a**). Both ventricular zone progenitors undergoing mitosis at the ventricular surface (**Fig. 3b**) and progenitors undergoing mitosis in the SVZ (**Fig. 3c**) extended a basal process during M phase (**Fig. 3d**), as seen by immunostaining for phosphorylated vimentin, a mitotic marker[24]. The latter basal process-bearing mitotic cells were indeed OSVZ (rather than ISVZ) progenitors, as virtually all of them expressed Pax6 (**Fig. 3e**,**g**) and <5% expressed Tbr2 (**Fig. 3f**,**g**). In addition, these data suggest that the Pax6 and Tbr2 double-positive progenitors in the human SVZ (**Fig. 1b**) belong to the ISVZ progenitor subpopulation.

Neither DiI labeling from the pial surface nor phosphovimentin immunostaining provided evidence for an apical process extending from OSVZ progenitors at M-phase (**Fig. 3c**,**e**,**f**). We next investigated whether OSVZ progenitors expressed markers found in the apical domain of ventricular zone progenitors, such as prominin-1 (CD133), an apical plasma membrane protein[25], Par3, which is associated with their apical cell cortex[26–28], and ZO-1, which is associated with apical adherens junctions[29]. All three apical domain markers were highly concentrated at or near the ventricular surface of the human 13-wpc cortical wall, as previously observed for the cortical wall of rodents, but not in the SVZ (**Supplementary Fig. 1**). *In situ* hybridization for *PROM1*

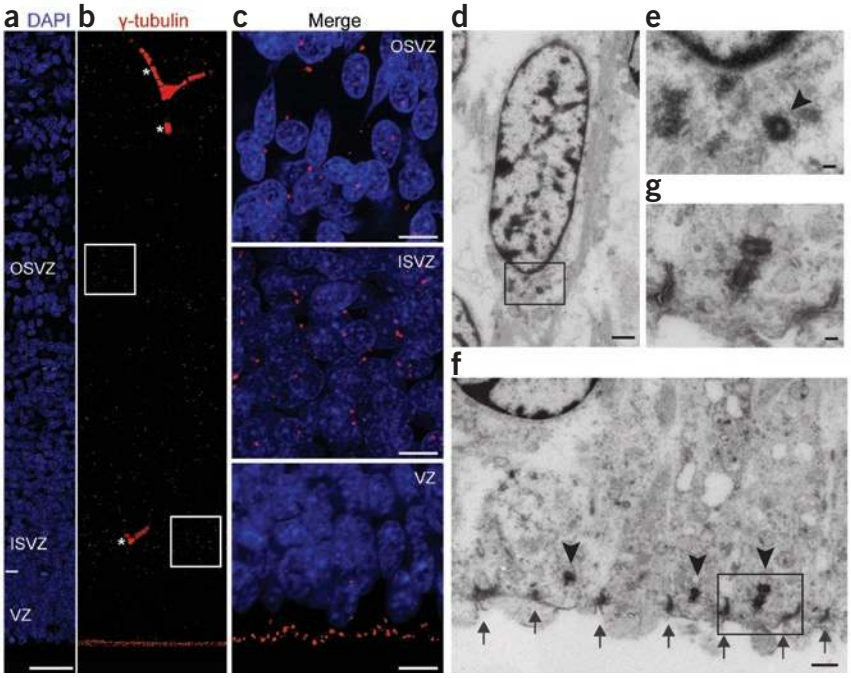

Figure 4 Human OSVZ progenitors have perinuclear centrosomes. (**a**–**c**) Immunofluorescence for γ-tubulin (red) on a cryosection of formalin-fixed 17-wpc human fetal neocortex. A stack of ten optical sections is shown in **a**, **b** and the top two panels of **c**. The bottom panel of **c** shows a stack of two optical sections. The DAPI image (**a**, blue) corresponds to a segment of the immunofluorescence image (**b**). Boxed areas in **b** are shown at higher magnification in (**c**, OSVZ) and (**c**, ISVZ), along with a higher magnification of the ventricular zone (**c**, VZ). Asterisks indicate autofluorescent blood vessels. Scale bars represent 50 μm (**a**,**b**) and 5 μm (**c**). (**d**–**g**) Electron microscopy of 17-wpc human fetal neocortex. The nucleus and perinuclear area of an OSVZ progenitor with a perinuclear centrosome is shown in **d**. The boxed area containing the centrosome is shown at higher magnification in **e** (arrowhead). A ventricular surface showing the apical region of several ventricular zone progenitors is displayed in **f**. Arrows indicate adherens junctions, the distance between which was measured to determine the average apical width (**Table 1**). Arrowheads indicate centrosomes. The boxed area containing a centrosome between adherens junctions is shown at higher magnification in **g**. The ventricular surface is down in **f** and **g**. Scale bars indicate 1 μm (**d**,**f**) and 200 nm (**e**,**g**).

mRNA indicated that human OSVZ progenitors, in contrast to ventricular zone progenitors, lacked prominin-1 expression (**Supplementary Fig. 2**). Together, these data indicate that human OSVZ progenitors have some, but not all, of the epithelial features of ventricular zone progenitors. They are polarized, extending a basal process to the basal lamina that is retained through M phase, but apparently lack an apical process at M phase and downregulate apical domain markers.

Perinuclear centrosomes in human OSVZ progenitors

We next analyzed the distribution of centrosomes in the human ventricular zone, ISVZ and OSVZ (**Fig. 4**). The centrosome marker γ-tubulin was abundantly expressed at the ventricular surface in 17-wpc human neocortex, with the remainder of the ventricular zone containing relatively few centrosomes (**Fig. 4a–c**), as seen previously in rodents[30]. Compared with the nonsurface region of the ventricular zone, centrosome abundance was increased in the human ISVZ and OSVZ and appeared to match that of the nuclei in these zones (**Fig. 4c**).

Quantification of centrosomes at the ventricular surface relative to apical endfeet by electron microscopy (**Fig. 4f**,**g**) revealed a 1:1 ratio (**Table 1**). Moreover, we observed at least one centrosome per OSVZ progenitor nucleus in interphase (**Table 1**), which was located in its immediate vicinity (**Fig. 4d**,**e**). Together, these data are consistent with the notion that essentially all apical centrosomes belong to ventricular zone progenitors (rather than both ventricular zone and OSVZ progenitors) and that OSVZ progenitors lack an apical process extending all the way to the ventricular surface, and imply that OSVZ progenitor nuclei can proceed to mitosis at their interphase location.

Human OSVZ progenitors show random cleavage orientation

Given that mouse basal progenitors lack apical-basal polarity in M phase and have a near-random cleavage plane orientation[8], our finding that human OSVZ progenitors in M phase exhibit basal polarity (**Fig. 3a–g**) raised the question whether they have a random cleavage plane orientation or, as with the basal process-bearing ventricular zone progenitors, an orientation that is predominantly parallel to their radial axis. We analyzed >100 mitotic human OSVZ progenitors and found a near-random orientation of their mitotic spindle, as deduced from the position of the sister chromatids at anaphase (**Fig. 5a,b**). The same result was obtained when Pax6-positive mitoses in the SVZ were analyzed for cleavage plane orientation (**Fig. 5c**). This was in contrast to mitotic human ventricular zone progenitors, the anaphase spindles of which showed a clear preference for an orientation that largely paralleled the ventricular surface (**Fig. 5a,b**), predicting a cleavage plane that was largely parallel to the radial, apical-basal axis of the cells, as has been known to be the case for the vast majority of rodent ventricular zone progenitors[4,6,27,31].

We analyzed >150 mitotic human ISVZ progenitors and found that they had a predicted cleavage plane orientation that was distinct from that of ventricular zone and OSVZ progenitors. Although there was

Table 1 Occurrence of centrosomes in the human ventricular zone and OSVZ

	Width (μm ± s.d.)	Number of 200-nm sections per cell	Probability of centrosome in region per section	Number of regions analyzed	Number of centrosomes observed	Occurrence of centrosome in region per section
Ventricular zone single-cell apical region	2.52 ± 1.03	13	1: 4.3	1419	318	1: 4.5
OSVZ perinuclear region	6.76 ± 1.47	34	1: 11.3	398	52	1: 7.7

Electron microscopy images of human 17-wpc telencephalon were analyzed. The number of 200-nm sections per cell refers to the average number of 200-nm sections that would be required to cover a ventricular zone single-cell apical region and an OSVZ perinuclear region. The probability of centrosome in region per section is the number of 200-nm sections divided by three, which is the number of 200-nm sections in which a ≥400-nm centrosome would appear. The occurrence of centrosome in region per section was obtained by dividing the number of regions analyzed by the number of centrosomes observed. For details, see Online Methods.

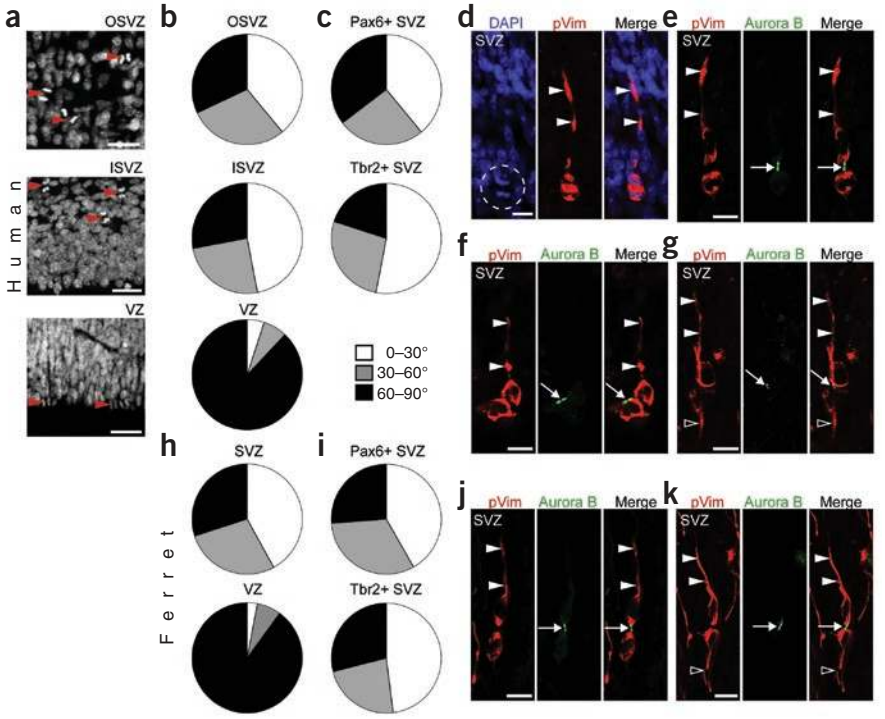

Figure 5 Human and ferret SVZ progenitors have near-random cleavage plane orientation, resulting in asymmetric inheritance of the basal process. (**a**) DAPI staining of paraffin sections of 14-wpc (top and bottom) and 16-wpc (middle) human fetal neocortex (formalin). Sister chromatids of progenitors in anaphase/early telophase (arrowheads) are visible in the OSVZ, ISVZ and ventricular zone (stacks of 4–8 optical sections). Scale bars represent 20 μm. (**b**,**c**) Quantification of cleavage plane orientation of progenitors in anaphase/early telophase. Cleavage plane orientations were grouped into three categories, 0–30° (white), 30–60° (gray) and 60–90° (black), with 0° corresponding to an orientation parallel to the ventricular surface. The total progenitors in OSVZ, ISVZ and ventricular zone (**b**) and the Pax6-positive and Tbr2-positive SVZ progenitors (**c**) in 14–16-wpc human neocortex (paraffin sections) are shown (**Supplementary Text**). (**d**–**g**) SVZ progenitors analyzed by immunofluorescence for phosphovimentin (pVim, red) on a vibratome section (**d**) and double immunofluorescence for phosphovimentin (pVim, red) and Aurora B (green) on cryosections (**e**–**g**) of 13-wpc fetal human neocortex (PFA, stacks of 5–12 optical sections). Dashed circle in **d** indicates DAPI-stained sister chromatids in anaphase. Solid arrowheads indicate phosphovimentin-positive basal processes, arrows indicate midbodies and open arrowheads indicate a phosphovimentin-positive apical process. Scale bars represent 5 μm. (**h**,**i**) Data are presented as in **b** and **c** for E39 ferret neocortex (PFA), except that the total progenitors in OSVZ and ISVZ were pooled (SVZ). (**j**,**k**) Data are presented as in **e**–**g** for E39 ferret neocortex (PFA, stacks of 4–6 optical sections).

a substantial (≥25%) contribution by the vertical (60–90°) and the oblique (30–60°) category of cleavage plane orientations, almost half of them fell into the horizontal (0–30°) category (**Fig. 5a**,**b**). The same result was obtained when we examined cleavage plane orientation of Tbr2-positive mitoses in the SVZ (**Fig. 5c**). This nonrandom cleavage plane orientation of ISVZ progenitors is reminiscent of that of rat[22] (but not mouse[8]) basal/intermediate progenitors.

The random cleavage plane orientation of OSVZ progenitors implies that the inheritance of their basal process and basally polarized cell fate determinants by the daughter cells will be asymmetric. Indeed, the basal process was inherited by one of the nascent daughter cells of dividing human OSVZ progenitors, as seen by phosphovimentin immunofluorescence (**Fig. 5d–g**). Occasionally, the other daughter cell, which was still connected to the former via the midbody, extended a process in the opposite, apical direction (**Fig. 5g**).

OSVZ progenitors exist in ferret neocortex

As human OSVZ progenitors are distinct from rodent basal progenitors, we asked whether OSVZ progenitors are specific to primates[9] or can be found in other brains with a gyrencephalic cerebral cortex. To investigate this possibility, we used the ferret, a gyrencephalic nonprimate. Specifically, we used embryonic day 32 (E32) ferret cortex, which corresponds approximately to human 10 wpc cortex, E39 ferret cortex, which corresponds approximately to human 14 wpc cortex, and postnatal day 10 (P10) ferret cortex, a late stage of neurogenesis at which the ferret cortex shows overt gyrencephaly[32,33]. We subjected the ferret cortex of these stages to the same analyses as human fetal neocortex.

The ferret SVZ was similar to the human SVZ and distinct from the rodent SVZ, with Pax6-positive nuclei progressively appearing in the SVZ at the expense of the ventricular zone (**Fig. 1n**,**p**,**r**) and Tbr2-positive nuclei being concentrated in the region of the embryonic SVZ that abutted on the ventricular zone (**Fig. 1o**,**q**,**s**). As in the developing human neocortex, the mitotic cells in the ferret ventricular zone were Pax6 positive (**Fig. 1l**) and largely Tbr2 negative (**Fig. 1l**), and the mitotic cells in the ferret SVZ were almost all Pax6 positive (**Fig. 1m**), with Tbr2 expression decreasing from ≈80% to ≈40% during cortical development (**Fig. 1m**).

Similarly, the cytoplasmic markers of ventricular zone progenitors and RGCs in rodents, nestin, GLAST and BLBP, were all expressed in the cell body of both the ventricular zone progenitors and SVZ progenitors in the E39 ferret neocortex (**Supplementary Fig. 3**); the main difference between the ferret neocortex and the fetal human neocortex being the lack of GFAP expression in the embryonic (but not postnatal) ferret neocortex (data not shown), as is the case for the early embryonic rodent neocortex[19]. These data indicate that a major subpopulation of ferret SVZ progenitors resemble human OSVZ progenitors. Using Nissl staining, we found cytoarchitectonically distinct zones in the ferret SVZ that were consistent with the existence of an ISVZ and OSVZ and a radial appearance of the progenitors in the outer region of the E39 ferret SVZ (data not shown), supporting the idea that a major portion of ferret SVZ progenitors are of the OSVZ type and are distinct from rodent basal progenitors.

Ferret OSVZ progenitors retain a basal process in M phase

We next determined whether ferret OSVZ progenitors extend basal processes and retain them through M phase. Using DiI labeling from the pial side of E39 cortical sections, we found that progenitors in the ferret SVZ, identifiable as cycling cells by Ki67 immunostaining (**Fig. 3i**), extended basal processes all the way to the pial surface and, in several of these cases, also had an apical process directed toward, but not reaching, the ventricular surface (**Fig. 3h**). Moreover, ferret OSVZ progenitors, similarly

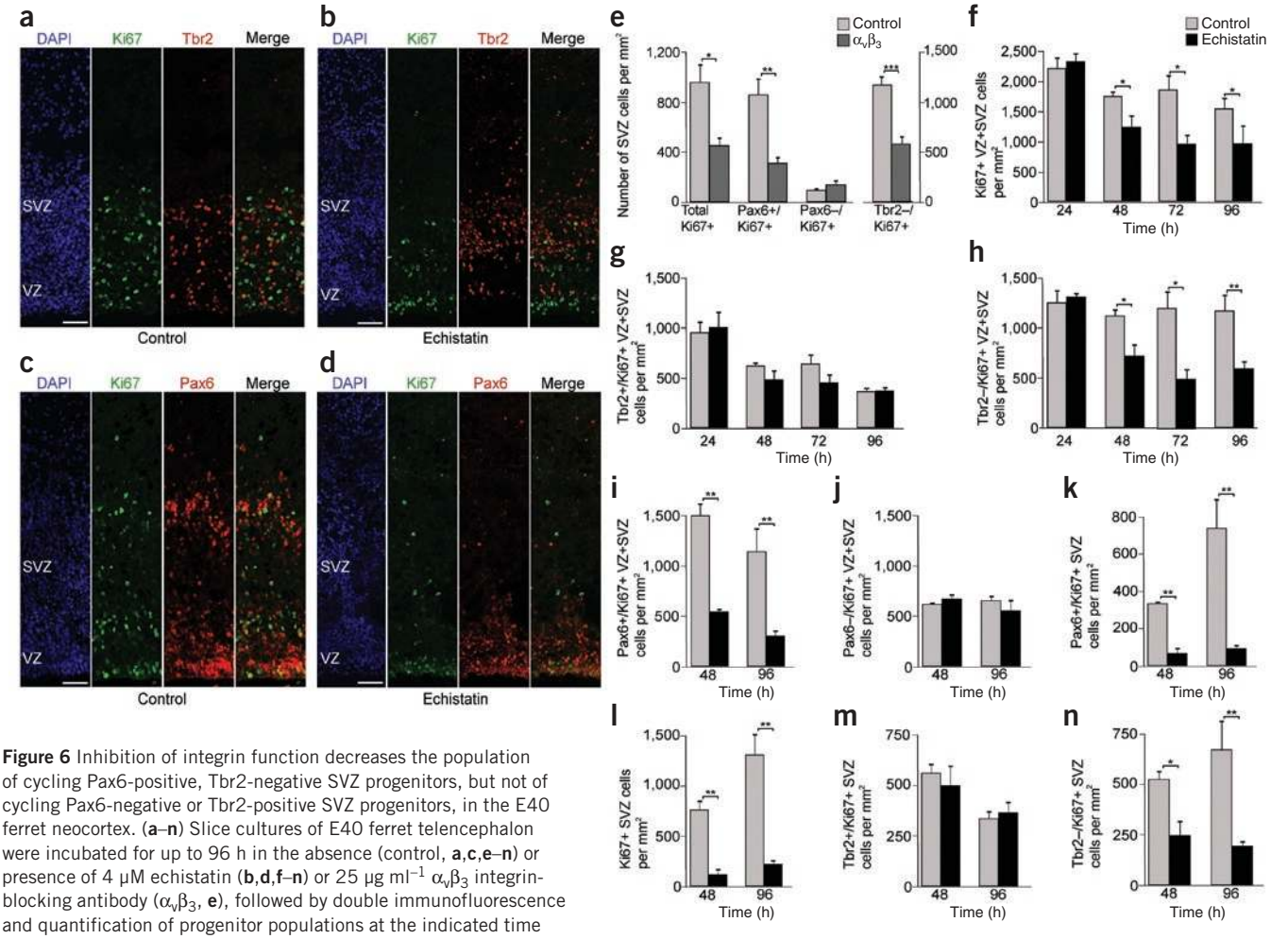

Figure 6 Inhibition of integrin function decreases the population of cycling Pax6-positive, Tbr2-negative SVZ progenitors, but not of cycling Pax6-negative or Tbr2-positive SVZ progenitors, in the E40 ferret neocortex. (**a**–**n**) Slice cultures of E40 ferret telencephalon were incubated for up to 96 h in the absence (control, **a**,**c**,**e**–**n**) or presence of 4 μM echistatin (**b**,**d**,**f**–**n**) or 25 μg ml^{-1} $\alpha_v\beta_3$ integrin-blocking antibody ($\alpha_v\beta_3$, **e**), followed by double immunofluorescence and quantification of progenitor populations at the indicated time points (**e**, 96 h). (**a**–**d**) Double immunofluorescence after 96 h of culture for Ki67 (green) and either Tbr2 (**a**,**b**, red) or Pax6 (**c**,**d**, red). DAPI staining is shown in blue. The top margin of the images corresponds to the transition zone subplate/cortical plate. Scale bars represent 50 μm. (**e**–**n**) Quantification of Ki67-positive progenitor populations, each expressed for 1 mm^2 of cortical wall from the ventricular surface (**f**–**j**, VZ + SVZ) or the ventricular zone/SVZ boundary (**e**,**k**–**n**, SVZ) to the beginning of the cortical plate: total Ki67-positive progenitors (**e**,**f**,**l**), Ki67-positive progenitors expressing Pax6 (**e**,**i**,**k**), Ki67-positive progenitors lacking Pax6 (**e**,**j**), Ki67-positive progenitors expressing Tbr2 (**g**,**m**), Ki67-positive progenitors lacking Tbr2 (**e**,**h**,**n**). Data in **f** are from double immunofluorescence for Tbr2 and data in **l** are from double immunofluorescence for Pax6 (**Supplementary Text**). Error bars indicate s.e.m. $^*P < 0.05$, $^{**}P < 0.01$ and $^{***}P < 0.001$.

to ventricular zone progenitors (**Fig. 3j**), retained their basal processes through M phase, as indicated by phosphovimentin immunostaining (**Fig. 3k**,**l**). Virtually all of these mitotic basal process–bearing ferret OSVZ progenitors were Pax6 positive (**Fig. 3m**,**o**) and Tbr2 negative (**Fig. 3n**,**o**), despite the presence of Tbr2-positive mitotic cell bodies in the ferret SVZ (**Fig. 1o**,**q**,**s**). In contrast to ferret OSVZ progenitors in interphase (**Fig. 3h**,**i**), however, we did not observe apical processes of any substantial length in mitotic ferret OSVZ progenitors (**Fig. 3k**,**m**,**n**). In addition, apical domain markers (Par3, aPKC, ZO-1) were prominently expressed in ferret ventricular zone, but not OSVZ, progenitors, as was seen for fetal human neocortex (**Supplementary Fig. 1**).

We conclude that the ferret SVZ, like the human SVZ, contains at least two progenitor populations. One comprises progenitors that resemble rodent basal progenitors in that they express Tbr2 and lack processes of any substantial length in mitosis and therefore appear to be unpolarized when undergoing cell division. These progenitors are found mostly in the region of the SVZ that abuts on the ventricular zone, consistent with the existence of an ISVZ in the ferret. The other ferret SVZ progenitor population comprises cells with features that are distinct from rodent basal progenitors, including maintenance of Pax6 and cytoplasmic ventricular zone progenitor marker expression and retention of a basal process through mitosis, which implies basal polarity in M phase. These progenitors are found throughout the ferret SVZ, are apparently sparser in the ISVZ and resemble human OSVZ progenitors.

We next analyzed the cleavage plane orientation of E39 ferret progenitors. The predicted cleavage planes of mitotic SVZ progenitors were distributed over all three categories of orientation, with a slight preference for a horizontal orientation (**Fig. 5h**). Separate analyses of Pax6-positive and Tbr2-positive ferret SVZ mitoses (**Fig. 5i**) indicated that the preference for a horizontal orientation was characteristic of the latter mitoses, with a near-random orientation of the former. This was in contrast to mitotic ventricular zone progenitors, ≈90% of which had a predicted cleavage plane orientation that largely paralleled the radial, apical-basal axis of the cells (**Fig. 5h**). Moreover, consistent with the data on cleavage plane orientation, the basal processes of mitotic ferret OSVZ progenitors were inherited by only one of the daughter cells (**Fig. 5j**,**k**), indicative of asymmetric division, as was found to be the case for human OSVZ progenitors (**Fig. 5d**–**g**).

OSVZ progenitors depend on integrin function

The finding that the ferret SVZ contains OSVZ progenitors, which have so far only been reported for primates[9], offered an experimental system for exploring the importance of their basal process retention and basal lamina contact. Specifically, we focused on integrin receptors[34–37]. Integrin function can be blocked by disintegrins, snake venoms that prevent ligand binding to certain, arginine-glycine-aspartate–sensitive integrins[38]. Integrins, notably integrin $\alpha_5\beta_1$ and α_v, are expressed on nestin-positive cortical progenitors (RGCs) in rodents[39,40]. We therefore examined the effects of echistatin, a disintegrin with high affinity for $\alpha_5\beta_1$ and $\alpha_v\beta_3$ integrins[41], on SVZ progenitors in organotypic slice cultures of E40 ferret telencephalon.

Exposure of E40 ferret neocortex for up to 4 d to 4 μM echistatin, a concentration previously used for neural stem cell cultures[42], substantially reduced the population size of cycling progenitors, as identified by Ki67 immunofluorescence (**Fig. 6**). This reduction was detected after 2–4 d of culture and was observed in both the ventricular zone and SVZ, but the magnitude of the reduction was greater for the SVZ (maximally 83%; **Fig. 6l**) than for the sum of ventricular zone and SVZ (maximally 48%; **Fig. 6f**). As the mitotic basal process–bearing ferret SVZ progenitors express Pax6 and not Tbr2, whereas mitotic Tbr2-positive SVZ progenitors only very rarely, if at all, have a basal process (**Fig. 3m–o**), we asked whether the reduction in Ki67-positive cells selectively affected the Pax6-positive and Tbr2-negative, but not the Tbr2-positive, progenitor subpopulation.

The Tbr2-positive subpopulation of Ki67-positive progenitors, analyzed in the sum of ventricular zone and SVZ (**Fig. 6g**) and in the SVZ alone (**Fig. 6m**), was largely unaffected by echistatin treatment, whereas the Tbr2-negative subpopulation was reduced by more than half (**Fig. 6h**,**n**). Consistent with this, the Pax6-positive subpopulation of Ki67-positive progenitors was markedly reduced by echistatin treatment (**Fig. 6i**), whereas the Pax6-negative subpopulation was essentially unaffected (**Fig. 6j**). Again, the magnitude of the reduction in the Pax6-positive and Tbr2-negative subpopulation was greater for the SVZ (maximally 87% for Pax6; **Fig. 6k**) than for the sum of ventricular zone and SVZ (maximally 73% for Pax6; **Fig. 6i**). These data indicate that interference with integrin function by exposure to disintegrins selectively reduces the population size of those ferret SVZ progenitors that retain a basal process throughout their cell cycle.

To corroborate these observations, we used blocking antibodies to target specific integrins. The addition of 25 μg ml^{-1} of antibody to $\alpha_v\beta_3$ integrin to organotypic slice cultures of E40 ferret telencephalon for 4 d markedly reduced the number of the total Ki67-positive, the Pax6 and Ki67 double-positive, and the Tbr2-negative and Ki67-positive progenitors in the SVZ, without affecting the Pax6-negative and Ki67-positive SVZ progenitors (**Fig. 6e**). We conclude that disruption of $\alpha_v\beta_3$ integrin function by blocking antibody reduces the population size of ferret OSVZ progenitors.

If the reduction in the Pax6-positive and Tbr2-negative subpopulation of ferret SVZ progenitors (OSVZ progenitors) that occurred after disintegrin treatment or addition of blocking antibody reflected basal process–mediated integrin function, one would expect the relevant integrin(s) to be present on the basal process of ferret SVZ progenitors. We therefore immunostained mitotic basal process–bearing E39 ferret SVZ progenitors for β3-integrin. Indeed, β3-integrin was detected in these processes, being concentrated in distal varicosities (**Fig. 7a**,**b**). Consistent with the close relationship between OSVZ and ventricular zone progenitors, we also found β3-integrin–positive varicosities on the basal process of ventricular zone progenitors (**Fig. 7c**,**d**). We conclude that retention of the basal process may endow OSVZ progenitors with the capacity for basal process–triggered integrin signaling, which is required for ensuring the full population size of these progenitors.

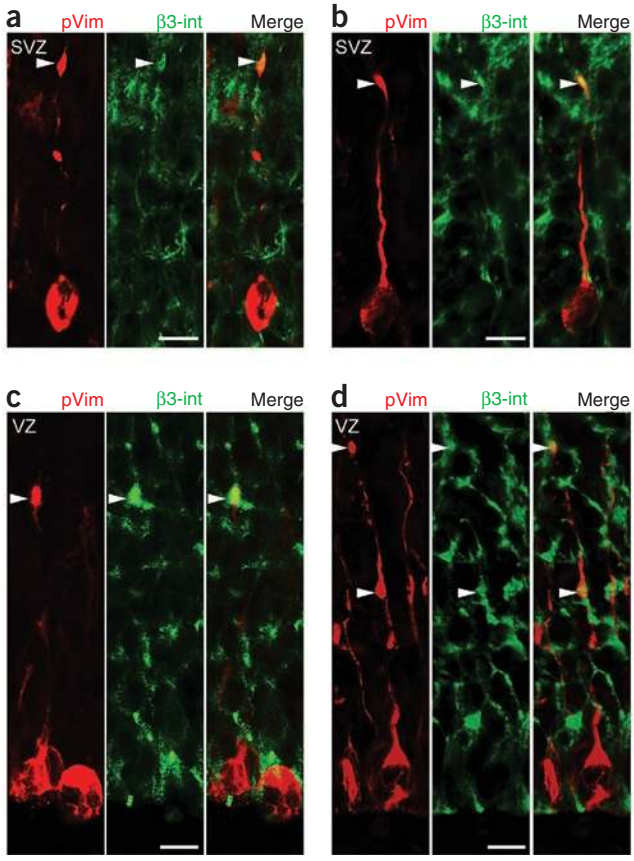

Figure 7 Localization of β3-integrin on basal processes of ferret SVZ and ventricular zone progenitors. (**a**–**d**) Double immunofluorescence for phosphovimentin (pVim, red) and β3-integrin (β3-int, green) on cryosections of E39 ferret neocortex, showing mitotic, basal process–bearing SVZ progenitors (**a**,**b**) and ventricular zone progenitors (**c**,**d**). Note the integrin immunoreactivity at varicosities of the basal process (arrowheads). Scale bars represent 5 μm.

DISCUSSION

OSVZ progenitors: a hallmark of a gyrencephalic cortex?

Our results identify a specific cell biological feature of neural progenitors that appears to be linked to a hallmark of neocortex expansion, the increase in the SVZ. Specifically, OSVZ progenitors in the developing, eventually gyrencephalic cortex of human and ferret differ from the SVZ progenitors of the lissencephalic rodent cortex in that they retain a basal process contacting the basal lamina throughout the cell cycle. This retention has important implications for the cell polarity of SVZ progenitors and whether their divisions are cell biologically symmetric or asymmetric, which may influence their capacity for self-renewal and could be important for the magnitude of their neuron output. Moreover, our results suggest a link between basal process retention and the signaling triggered by basal lamina and related extracellular matrix proteins, as integrin function was required for OSVZ progenitor proliferation.

It was previously suggested[9] that the OSVZ may be primate specific. Our findings indicate that OSVZ progenitors exist in a nonprimate species, the ferret, which also develops a gyrencephalic cortex. These data suggest that OSVZ progenitors (delaminated RGCs retaining basal lamina contact) may be characteristic of a developing gyrencephalic cortex and that it is a quantitative, rather than a qualitative, aspect (the relative abundance of OSVZ progenitors) that distinguishes the developing primate from the developing gyrencephalic nonprimate cortex.

OSVZ progenitors are delaminated epithelial-like RGCs

Like rodent basal progenitors, human and ferret OSVZ progenitors delaminate from the apical adherens junction belt, retract their apical process and downregulate apical polarity markers. However, OSVZ progenitors are different from the typical rodent basal progenitor in that they retain characteristic features of RGCs: sustained expression of Pax6 and several cytoplasmic RGC markers[43] and a basal process through M phase. Consistent with previous findings[9], OSVZ progenitors can therefore be regarded as delaminated RGCs, a conclusion reported independently[44] while our manuscript was under review. Notably, OSVZ progenitors retain, via their basal process, cell polarity and a canonical epithelial feature, the contact with the basal lamina. Our findings support the epithelial progenitor hypothesis[4].

However, given the downregulation of apical polarity and loss of apical adherens junctions, OSVZ progenitors apparently do not retain all possible epithelial features. It should be noted that, concomitant with the loss of apical polarity, neural progenitors in general switch from a predominantly vertical (apical progenitors) to a near-random, if not preferentially horizontal (all basally dividing progenitors), cleavage plane orientation. Symmetric proliferative divisions of polarized neural progenitors thus appear to be linked to the maintenance of bipolar (apical-basal) cell polarity, whereas the transition to monopolar (basal) cell polarity seems to confine neural progenitors to cell biologically asymmetric divisions (**Supplementary Fig. 4**).

Basal polarity, asymmetric cell division and neuron output

Rodent basal progenitors in M phase are nonpolarized, and their divisions can only be symmetric (in cell biological terms) and do not require any particular control of cleavage plane orientation[8]. In contrast, apical progenitors exhibit extreme apical-basal polarity, and for their divisions to be symmetric, two requirements must be met: the cleavage plane must be oriented perfectly parallel to the apical-basal cell axis, and the cleavage must divide apical and basal cell constituents[6]. Mechanisms that meet either requirement have been reported[4,21,45]. Our findings that human and ferret OSVZ progenitors, similarly to mouse basal progenitors, have a near-random cleavage plane orientation, but, in contrast to mouse basal progenitors, retain basal polarity, imply that OSVZ progenitor divisions are cell biologically asymmetric. Given that both rodent basal progenitors and human/ferret OSVZ progenitors have random cleavage plane orientation, the retention of the basal process in OSVZ progenitors converts them from dividing symmetrically (as rodent basal progenitors do) to dividing asymmetrically (**Supplementary Fig. 4**).

Repeated asymmetric divisions of apical progenitors and the OSVZ progenitors generated from them would considerably affect neuron output. The existence of basal progenitors undergoing symmetric, neurogenic and self-consuming, divisions merely doubles the number of neurons generated per apical progenitor division (**Supplementary Fig. 4**). In contrast, repeated asymmetric, neurogenic and self-renewing, OSVZ progenitor divisions would result in the progressive accumulation of neurons, outnumbering that in the apical progenitor–to–basal progenitor lineage (**Supplementary Fig. 4**).

Integrins on basal processes and OSVZ progenitor expansion

Thus, the crucial question arising is: why are OSVZ progenitors, in contrast to most basal progenitors in the rodent, capable of undergoing self-renewing divisions, as has been seen previously[23]. Our data suggest that the answer to this question lies in the cell biological difference between these two types of progenitors, the retention of the basal process. Stem cells in other epithelial systems, such as the skin, characteristically maintain basal lamina contact[46,47]. Moreover, the basal process has recently been implicated in the self-renewal of mouse apical progenitors[31]. Extrapolating from these results, we hypothesize that OSVZ progenitors maintain stem cell–like properties via their basal process and the basal lamina contact it mediates.

One of the major signaling pathways by which basal lamina and related extracellular matrix proteins influence cell fate involves integrin receptors. Indeed, our data indicate that integrins, which are present in the basal process[39,40], are required for OSVZ progenitor proliferation. Notably, two independent forms of interference with integrin function selectively reduced the population size of ferret OSVZ progenitors (Pax6 positive, Tbr2 negative), which retained their basal process throughout the cell cycle, whereas no such effects were observed for the SVZ progenitor subpopulation that lacked basal processes (Pax6 negative, Tbr2 positive). Given our observation that β3-integrins are concentrated at varicosities of the basal process of SVZ progenitors, it is possible that basal process retention serves to allow integrin-mediated self-renewal of SVZ progenitors. This concept is not necessarily contradicted by previous findings that perturbation of integrin function in mouse RGCs does not substantially impair their self-renewal[35], as the latter progenitors have access to potential proliferation signals from the ventricle, which OSVZ progenitors do not. In conclusion, our results suggest that basal process–based integrin function is important for SVZ expansion during cortex evolution.

METHODS

Methods and any associated references are available in the online version of the paper at http://www.nature.com/natureneuroscience/.

Note: Supplementary information is available on the Nature Neuroscience website.

ACKNOWLEDGMENTS

We thank J. Helppi and other members of the animal facility, and the light microscopy facility, of the Max Planck Institute of Molecular Cell Biology and Genetics for excellent support, A.-M. Marzesco and E. Taverna for experimental advice, C. Haffner for excellent technical assistance, S. Preibisch for developing the Fiji plug-in, and J. Pulvers for his helpful comments on the manuscript. We are grateful to the Bundesinstitut für Risikobewertung and Biotie Therapies for ferret housing. S.A.F., I.K. and J.L.F. were members of the International Max Planck Research School for Molecular Cell Biology and Bioengineering. W.B.H. was supported by a grant from the Deutsche Forschungsgemeinschaft (DFG) (SFB 655, A2) and by the DFG-funded Center for Regenerative Therapies Dresden and by the Fonds der Chemischen Industrie.

AUTHOR CONTRIBUTIONS

S.A.F. performed the experiments on human tissue. S.A.F. and I.K. contributed equally to the experiments on ferret tissue and co-wrote the paper. J.V. provided human tissue and gave advice on the experiments. M.W.-B. performed the electron microscopy analyses. D.S. proposed the use of echistatin and contributed to some experiments. D.C. provided reagents for prominin-1 analyses. J.L.F., A.R., W.D. and R.N. provided human tissue. W.B.H. supervised the project and wrote the paper.

COMPETING FINANCIAL INTERESTS

The authors declare no competing financial interests.

Published online at http://www.nature.com/natureneuroscience/.
Reprints and permissions information is available online at http://www.nature.com/reprintsandpermissions/.

1. Kriegstein, A., Noctor, S. & Martínez-Cerdeño, V. Patterns of neural stem and progenitor cell division may underlie evolutionary cortical expansion. *Nat. Rev. Neurosci.* **7**, 883–890 (2006).
2. Molnár, Z. *et al.* Comparative aspects of cerebral cortical development. *Eur. J. Neurosci.* **23**, 921–934 (2006).
3. Abdel-Mannan, O., Cheung, A.F. & Molnár, Z. Evolution of cortical neurogenesis. *Brain Res. Bull.* **75**, 398–404 (2008).
4. Fish, J.L., Kennedy, H., Dehay, C. & Huttner, W.B. Making bigger brains—the evolution of neural progenitor cell division. *J. Cell Sci.* **121**, 2783–2793 (2008).
5. Rakic, P. Evolution of the neocortex: a perspective from developmental biology. *Nat. Rev. Neurosci.* **10**, 724–735 (2009).
6. Götz, M. & Huttner, W.B. The cell biology of neurogenesis. *Nat. Rev. Mol. Cell Biol.* **6**, 777–788 (2005).

7. Kriegstein, A. & Alvarez-Buylla, A. The glial nature of embryonic and adult neural stem cells. *Annu. Rev. Neurosci.* **32**, 149–184 (2009).
8. Attardo, A., Calegari, F., Haubensak, W., Wilsch-Bräuninger, M. & Huttner, W.B. Live imaging at the onset of cortical neurogenesis reveals differential appearance of the neuronal phenotype in apical versus basal progenitor progeny. *PLoS One* **3**, e2388 (2008).
9. Smart, I.H., Dehay, C., Giroud, P., Berland, M. & Kennedy, H. Unique morphological features of the proliferative zones and postmitotic compartments of the neural epithelium giving rise to striate and extrastriate cortex in the monkey. *Cereb. Cortex* **12**, 37–53 (2002).
10. Murphy, W.J., Pringle, T.H., Crider, T.A., Springer, M.S. & Miller, W. Using genomic data to unravel the root of the placental mammal phylogeny. *Genome Res.* **17**, 413–421 (2007).
11. Englund, C. *et al.* Pax6, Tbr2, and Tbr1 are expressed sequentially by radial glia, intermediate progenitor cells and postmitotic neurons in developing neocortex. *J. Neurosci.* **25**, 247–251 (2005).
12. Kowalczyk, T. *et al.* Intermediate neuronal progenitors (basal progenitors) produce pyramidal-projection neurons for all layers of cerebral cortex. *Cereb. Cortex* **19**, 2439–2450 (2009).
13. Bayatti, N. *et al.* A molecular neuroanatomical study of the developing human neocortex from 8 to 17 postconceptional weeks revealing the early differentiation of the subplate and subventricular zone. *Cereb. Cortex* **18**, 1536–1548 (2008).
14. Götz, M., Stoykova, A. & Gruss, P. Pax6 controls radial glia differentiation in the cerebral cortex. *Neuron* **21**, 1031–1044 (1998).
15. Mo, Z. & Zecevic, N. Is Pax6 critical for neurogenesis in the human fetal brain? *Cereb. Cortex* **18**, 1455–1465 (2008).
16. Carney, R.S., Bystron, I., Lopez-Bendito, G. & Molnár, Z. Comparative analysis of extra-ventricular mitoses at early stages of cortical development in rat and human. *Brain Struct. Funct.* **212**, 37–54 (2007).
17. Kriegstein, A.R. & Götz, M. Radial glia diversity: a matter of cell fate. *Glia* **43**, 37–43 (2003).
18. Levitt, P. & Rakic, P. Immunoperoxidase localization of glial fibrillary acidic protein in radial glial cells and astrocytes of the developing rhesus monkey brain. *J. Comp. Neurol.* **193**, 815–840 (1980).
19. Woodhams, P.L., Bascó, E., Hajós, F., Csillág, A. & Balázs, R. Radial glia in the developing mouse cerebral cortex and hippocampus. *Anat. Embryol. (Berl.)* **163**, 331–343 (1981).
20. Miyata, T., Kawaguchi, A., Okano, H. & Ogawa, M. Asymmetric inheritance of radial glial fibers by cortical neurons. *Neuron* **31**, 727–741 (2001).
21. Kosodo, Y. *et al.* Cytokinesis of neuroepithelial cells can divide their basal process before anaphase. *EMBO J.* **27**, 3151–3163 (2008).
22. Noctor, S.C., Martínez-Cerdeño, V. & Kriegstein, A.R. Distinct behaviors of neural stem and progenitor cells underlie cortical neurogenesis. *J. Comp. Neurol.* **508**, 28–44 (2008).
23. Lukaszewicz, A. *et al.* G1 phase regulation, area-specific cell cycle control, and cytoarchitectonics in the primate cortex. *Neuron* **47**, 353–364 (2005).
24. Kamei, Y. *et al.* Visualization of mitotic radial glial lineage cells in the developing rat brain by Cdc2 kinase–phosphorylated vimentin. *Glia* **23**, 191–199 (1998).
25. Weigmann, A., Corbeil, D., Hellwig, A. & Huttner, W.B. Prominin, a novel microvilli-specific polytopic membrane protein of the apical surface of epithelial cells, is targeted to plasmalemmal protrusions of non-epithelial cells. *Proc. Natl. Acad. Sci. USA* **94**, 12425–12430 (1997).
26. Manabe, N. *et al.* Association of ASIP/mPAR-3 with adherens junctions of mouse neuroepithelial cells. *Dev. Dyn.* **225**, 61–69 (2002).
27. Kosodo, Y. *et al.* Asymmetric distribution of the apical plasma membrane during neurogenic divisions of mammalian neuroepithelial cells. *EMBO J.* **23**, 2314–2324 (2004).
28. Costa, M.R., Wen, G., Lepier, A., Schroeder, T. & Götz, M. Par-complex proteins promote proliferative progenitor divisions in the developing mouse cerebral cortex. *Development* **135**, 11–22 (2008).
29. Aaku-Saraste, E., Hellwig, A. & Huttner, W.B. Loss of occludin and functional tight junctions, but not ZO-1, during neural tube closure—remodeling of the neuroepithelium prior to neurogenesis. *Dev. Biol.* **180**, 664–679 (1996).
30. Chenn, A., Zhang, Y.A., Chang, B.T. & McConnell, S.K. Intrinsic polarity of mammalian neuroepithelial cells. *Mol. Cell. Neurosci.* **11**, 183–193 (1998).
31. Konno, D. *et al.* Neuroepithelial progenitors undergo LGN-dependent planar divisions to maintain self-renewability during mammalian neurogenesis. *Nat. Cell Biol.* **10**, 93–101 (2008).
32. Smart, I.H. & McSherry, G.M. Gyrus formation in the cerebral cortex in the ferret. I. Description of the external changes. *J. Anat.* **146**, 141–152 (1986).
33. Neal, J. *et al.* Insights into the gyrification of developing ferret brain by magnetic resonance imaging. *J. Anat.* **210**, 66–77 (2007).
34. Schmid, R.S. & Anton, E.S. Role of integrins in the development of the cerebral cortex. *Cereb. Cortex* **13**, 219–224 (2003).
35. Haubst, N., Georges-Labouesse, E., De Arcangelis, A., Mayer, U. & Gotz, M. Basement membrane attachment is dispensable for radial glial cell fate and for proliferation, but affects positioning of neuronal subtypes. *Development* **133**, 3245–3254 (2006).
36. Lathia, J.D., Rao, M.S., Mattson, M.P. & Ffrench-Constant, C. The microenvironment of the embryonic neural stem cell: lessons from adult niches? *Dev. Dyn.* **236**, 3267–3282 (2007).
37. Radakovits, R., Barros, C.S., Belvindrah, R., Patton, B. & Müller, U. Regulation of radial glial survival by signals from the meninges. *J. Neurosci.* **29**, 7694–7705 (2009).
38. Calvete, J.J. *et al.* Snake venom disintegrins: evolution of structure and function. *Toxicon* **45**, 1063–1074 (2005).
39. Hirsch, E. *et al.* Alpha v integrin subunit is predominantly located in nervous tissue and skeletal muscle during mouse development. *Dev. Dyn.* **201**, 108–120 (1994).
40. Yoshida, N. *et al.* Decrease in expression of alpha 5 beta 1 integrin during neuronal differentiation of cortical progenitor cells. *Exp. Cell Res.* **287**, 262–271 (2003).
41. Wierzbicka-Patynowski, I. *et al.* Structural requirements of echistatin for the recognition of alpha(v)beta(3) and alpha(5)beta(1) integrins. *J. Biol. Chem.* **274**, 37809–37814 (1999).
42. Flanagan, L.A., Rebaza, L.M., Derzic, S., Schwartz, P.H. & Monuki, E.S. Regulation of human neural precursor cells by laminin and integrins. *J. Neurosci. Res.* **83**, 845–856 (2006).
43. Middeldorp, J. *et al.* GFAPdelta in radial glia and subventricular zone progenitors in the developing human cortex. *Development* **137**, 313–321 (2010).
44. Hansen, D.V., Lui, J.H., Parker, P.R. & Kriegstein, A.R. Neurogenic radial glia in the outer subventricular zone of human neocortex. *Nature* **464**, 554–561 (2010).
45. Fish, J.L., Kosodo, Y., Enard, W., Pääbo, S. & Huttner, W.B. Aspm specifically maintains symmetric proliferative divisions of neuroepithelial cells. *Proc. Natl. Acad. Sci. USA* **103**, 10438–10443 (2006).
46. Lechler, T. & Fuchs, E. Asymmetric cell divisions promote stratification and differentiation of mammalian skin. *Nature* **437**, 275–280 (2005).
47. Fuchs, E. Finding one's niche in the skin. *Cell Stem Cell* **4**, 499–502 (2009).

ONLINE METHODS

Tissue. Human fetal brain tissue was obtained from the Institut für Zell- und Neurobiologie, Centrum für Anatomie, Charité Berlin and the Klinik und Poliklinik für Frauenheilkunde und Geburtshilfe, Universitätsklinikum Carl Gustav Carus of the Technische Universität Dresden. The age of the human fetuses ranged from 10 to 17 wpc (10 wpc, $n = 1$; 11 wpc, $n = 1$; 12 wpc, $n = 1$; 13 wpc, $n = 1$; 14 wpc, $n = 2$; 16 wpc, $n = 2$; 17 wpc, $n = 1$), as assessed by ultrasound measurements of crown-rump length and other standard criteria of developmental stage determination. Pregnancies were terminated on the basis of social or medical indications. In the case of the latter, only medical indications known to not affect brain development (for example, amnion infection) were included. Human fetal brain tissue was obtained with informed written maternal consent, with approval of the local University Hospital Ethical Review Committees. Human fetuses were placed at 4 °C immediately after abortion and brains were dissected in ice-cold phosphate-buffered saline (PBS) and fixed for at least 24 h at 4 °C in either 4% PFA (wt/vol) in 120 mM phosphate buffer (pH 7.4, for cryosections and vibratome sections) or 4% formalin (wt/vol) in 100 mM phosphate buffer (pH 7.4, for paraffin sections, cryosections and vibratome sections).

Timed-pregnant ferrets were obtained from Marshall BioResources and housed at the Bundesinstitut für Risikobewertung or at Biotie Therapies. At E32, E39 or E40, pregnant ferrets were anesthetized by intramuscular injection of ketamine (20 mg per kg of body weight, Bela-Pharm) and xylazine (1 mg per kg, Pharma-Partner) and killed by intracardiac injection of T-61 (0.3 ml kg^{-1}, Intervet), followed by the immediate removal of embryos and dissection of the brains in ice-cold PBS. P10 ferrets were anesthetized by intraperitoneal injection of ketamine and xylazine and decapitated, followed by dissection of the brains. Embryonic and postnatal ferret brains were fixed in 4% PFA (E32, E39 and P10) or used for the preparation of slice cultures (E40). All animal experiments were performed in accordance with German animal welfare legislation and were approved by the Landesamt für Gesundheit und Soziales Berlin and the Landesdirektion Dresden.

Organotypic ferret cortical slice culture. E40 ferrets were dissected in Tyrode's solution at 4 °C. Brains were embedded in 3% low-melting agarose (Invitrogen, UltraPure) in PBS and cooled to 4 °C for vibratome sectioning. Sections (500 µm) of telencephalon were immersed at 4 °C in 1 ml per section of 1.5 mg ml^{-1} type Ia collagen (Cellmatrix, Nitta Gelatin) in DMEM in a 35-mm glass-bottom microwell dish (MatTek). Dishes were incubated for 5–10 min at 37 °C to allow the collagen to solidify, transferred to a humidified POC Chamber System gassed with 40% O_2, 5% CO_2 and 55% N_2 at 37 °C, and incubated for 30 min. We then added 2 ml of Neurobasal medium (Invitrogen) supplemented with 10% heat-inactivated horse serum (vol/vol Sigma), 1× N2 supplement (Invitrogen), 1× B27 supplement (Invitrogen), 2 mM L-glutamine and 100 U ml^{-1} penicillin/streptomycin, which defined the start of culture. In the case of perturbation of integrin signaling, 4 µM echistatin[42] (Sigma) or 25 µg ml^{-1} $\alpha_v\beta_3$ integrin blocking antibody (Millipore, MAB1976Z) was added to both the collagen/DMEM and the culture medium. Medium was changed after 48 h. The collagen-embedded sections were fixed by addition of 4% PFA in PBS for 24 h at 4 °C, followed by removal of the sections from the collagen, infiltration with 30% sucrose (wt/vol) for 48 h at 18–22 °C, and processing for cryosectioning and immunocytochemistry.

Immunocytochemistry. Human and ferret telencephalon was sectioned. For cryosectioning, fixed brain tissue was infiltrated with 30% sucrose in PBS overnight at 4 °C (except for E40 ferret slices) and then embedded in Tissue-Tek (Sakura Finetek) and stored at –20 °C. Cryostat sections were cut at 12–14 µm, except for E40 ferret slice cultures, which were cut at 16 µm. For vibratome sectioning, fixed brain tissue was embedded in 3% low-melting agarose in PBS, cut at 50 µm and stored in PBS at 4 °C until further processing. For microtome sectioning, formalin-fixed brain tissue was dehydrated in graded ethanol solutions, followed by xylene or chloroform, and then embedded in paraffin. Paraffin sections were cut at 12 µm, dewaxed in xylene and rehydrated in graded ethanol solutions. All sections were subjected to an antigen retrieval protocol. Cryosections and paraffin sections on glass slides were boiled for 1 min in a microwave oven at 800 W in citrate buffer (pH 6, Target Retrieval Solution, DakoCytomation), followed by 10 min at 80 W. Floating vibratome sections were heated in the same buffer for 30 min at 85 °C. Sections were then permeabilized with 0.3% Triton X-100 (wt/vol), quenched with 0.1 M glycine and then subjected to immunocytochemistry according to standard procedures[27]. Primary antibodies were incubated overnight (cryosections, vibratome sections) or for 1.5 d (paraffin sections) at 4 °C and secondary antibodies were incubated for 1 h at 18–22 °C. For primary antibodies, we used rabbit antibodies to Pax6 (Covance, PRB-278P, 1:200 for cryosections, 1:50 for paraffin sections), Tbr2 (Abcam, ab23345, 1:200 for cryosections, 1:50 for paraffin sections), PH3 (Millipore, 06-570, 1:200) conjugated to DyLight 633 (Thermo Scientific), nestin (Abcam, ab5968, 1:200), BLBP (Santa Cruz, sc-30088, 1:200), Par3 (Millipore, 07-330, 1:50), GLAST (Invitrogen, 428100, 1:200), Aurora B (Abcam, ab2254, 1:200) and β3-integrin (Abcam, ab75872, 1:200), and mouse monoclonal antibodies to human prominin-1 (80B258 (ref. 48), 8.7 ng μl^{-1}), aPKC (BD Transduction Laboratories, 610207, 1:100), ZO-1 (Invitrogen, 33-9100, 1:200), Ki67 antigen (DakoCytomation, M 7240, 1:200), GFAP (Sigma, G3893, 1:200), GLAST (Abcam, ab49643, 1:200) and phosphovimentin (Abcam, ab22651, 1:50; MBL, D076-3, 1:50). Goat Cy2-, Cy3- or Cy5-labeled secondary antibodies (Jackson Laboratories) were used (1:500). All sections were counterstained with DAPI (Sigma, 1:500) and mounted in Mowiol (Merck Biosciences).

DiI labeling. Human and ferret vibratome sections of PFA-fixed telencephalon were kept in 35-mm plastic microwell dishes (Nunc) in PBS and immobilized using a metal grid (diameter, 1 cm) with nylon wires (Warner Instruments). DiI suspension (10 µg μl^{-1} in ethanol, Molecular Probes) was applied to the section locally at the apical or basal side of the cortical wall using a glass capillary (0.5–1-µm opening) and an Eppendorf Transjector (model 5246) attached to an InjectMan NI2 micromanipulator under microscopic control (Axiovert 200, Zeiss). Sections were incubated for 5 d at 37 °C. Sections were then heated in citrate buffer (pH 6, Target Retrieval Solution, DakoCytomation) for 30 min at 85 °C, quenched with 0.1 M glycine and then subjected to immunocytochemistry, but without Triton X-100.

***In situ* hybridization.** *In situ* hybridization for human prominin-1 was performed according to standard methods, using cryosections and digoxigenin-labeled (DIG-RNA labeling kit, Roche) cRNA antisense and sense probes corresponding to the first 275 nucleotides of the open reading frame[49] at 100 ng ml^{-1}.

Image acquisition. Fluorescence and *in situ* hybridization images were acquired using a Zeiss 510 confocal laser-scanning microscope or an Olympus IX-71 wide-field microscope, using 20× or 40× objectives with either microscope. Images were acquired as 1-µm single optical sections and all panels shown are single 1-µm optical sections unless indicated otherwise. Single images were stitched together using Fiji software (http://pacific.mpi-cbg.de) and a plug-in[50]. All images were processed using Photoshop software (Adobe). All images are oriented with the ventricular surface down or with the bottom margin toward the ventricular surface.

Electron microscopy. For electron microscopy analysis, a vibratome section of formalin-fixed 17-wpc human telencephalon was postfixed in 2.5% glutaraldehyde (vol/vol) in 0.1 M sodium phosphate buffer (pH 7.4) and subsequently in 1% (wt/vol) osmium tetroxide before embedding in EmBed-812 (Science Services) according to standard procedures. Ultrathin 200-nm sections were cut on a Leica UCT ultramicrotome (Leica Microsystems), post-stained with uranyl acetate and lead citrate and viewed in a Tecnai 12 electron microscope (FEI). Images were taken with a Tietz F214 camera (TVIPS).

Quantification of centrosomes. For quantification of the occurrence of centrosomes in ventricular zone and OSVZ cells in interphase, electron microscopy images were analyzed as follows. The average width of the apical process of a cell contacting the ventricle (ventricular zone single-cell apical region) was defined as the distance between the apical-most features of cross-sectioned adherens junctions. The average width of the perinuclear region of an OSVZ cell (OSVZ perinuclear region) was defined as the diameter of their elongated, radially aligned nucleus perpendicular to the radial axis, assuming a negligible contribution of cytoplasm to the cell width. These distance measurements were performed using iTEM software (Olympus). The resulting values were used to calculate the average number of 200-nm sections that would be required to cover

 doi:10.1038/nn.2553

a ventricular zone single-cell apical region and an OSVZ perinuclear region. We assumed a centrosome size of ≥400 nm, which implies that a centrosome appears in three 200-nm sections (as a 400-nm centrosome will only rarely be contained in just two 200-nm sections).

Determination of cleavage plane orientation. Cleavage plane orientation of progenitors in the ventricular zone, ISVZ and OSVZ was deduced from the position of the DAPI-stained sister chromatids in anaphase or early telophase[27] and was expressed relative to the ventricular surface, with a cleavage plane parallel to the ventricular surface being defined as 0°.

Quantifications and statistical analysis. In the case of 16- and 17-wpc human neocortex, the basal-most region of the ventricular zone and the apical-most region of the OSVZ were distinguished from the interjacent ISVZ by the shape of DAPI-stained nuclei (radially elongated shape and radial orientation in the ventricular zone and OSVZ, spherical shape in the ISVZ[9]). The same criteria were applied to determine the boundary between the 10–14-wpc human and E32–P10 ferret ventricular zone (elongated nuclei) and SVZ (spherical nuclei). Quantification of cells for the parameters indicated was performed using Photoshop and ImageJ (US National Institutes of Health) or Fiji software. The length of the ventricular surface was determined by tracing it using ImageJ or Fiji software. For the determination of cortical wall area (excluding the cortical plate), a polygon was constructed using ImageJ and its area was calculated; the bottom and top side of the polygon corresponded to the traced ventricular surface and a straight line at the transition of the subplate to cortical plate, respectively, with the left and right side being two parallel straight lines in the radial axis of the cortical wall. Statistical significance was calculated using Student's *t* test.

48. Karbanová, J. *et al.* The stem cell marker CD133 (Prominin-1) is expressed in various human glandular epithelia. *J. Histochem. Cytochem.* **56**, 977–993 (2008).
49. Giebel, B. *et al.* Segregation of lipid raft markers including CD133 in polarized human hematopoietic stem and progenitor cells. *Blood* **104**, 2332–2338 (2004).
50. Preibisch, S., Saalfeld, S. & Tomancak, P. Globally optimal stitching of tiled 3D microscopic image acquisitions. *Bioinformatics* **25**, 1463–1465 (2009).